Journal of Energy Storage 34 (2021) 102200

Contents lists available at ScienceDirect

Journal of Energy Storage

journal homepage: www.elsevier.com/locate/est

Extra-Durable Hybrid Supercapacitor Based on Cobalt Sulfide and Carbon (MWCNT) Matrix Electrodes

I. Rathinamala [a,*], I. Manohara Babu [b], J. Johnson William [c], G. Muralidharan [c], N. Prithivikumaran [d]

[a] Department of Physics, V. V. Vanniaperumal College for Women (Autonomous), Virudhunagar, Tamilnadu, India
[b] Department of Physics, V. S. B. Engineering College, Karur, Tamilnadu, India
[c] Department of Physics, The Gandhigram Rural Institute - Deemed to be University, Gandhigram-624302, Tamilnadu, India
[d] Department of Physics, V.H.N. Senthikumara Nadar College (Autonomous), Virudhunagar, Tamilnadu, India

ARTICLE INFO

Keywords:
Multi-walled carbon nanotube
cobalt sulfide
hybrid
nanosheets
supercapacitor

ABSTRACT

A novel energy storage gadget with instantaneous energy/power density is significant in current scenario due to the rapid utilization of renewable energy sources. Also, the electrochemical property of the chosen electrodes have chiefly dependent on the structure of the electrode materials. Keeping these aspects in mind, we have devised to fabricate a hybrid supercapacitor (HSC) composed of a battery-type Faradic electrode (for energy source) and non-Faradic electrode (for power source). The composite electrode material (CoS_2/multi-walled carbon nanotube (MWCNT)) prepared in the present study having unique nanostructure (composed of nanosheets and nanotubes) provides plenty of channels for ion mobilization and results in excellent electrochemical performance. Moreover, the fabricated HSC (CoS_2/MWCNT//polypropylene & KOH//MWCNT) could capable of delivering an ultra-high specific energy of 8.16 W h kg^{-1} with a specific power of 696 W kg^{-1} at a specific current of 5 A g^{-1}. These positive features enriched with the prepared nanocomposite (CoS_2/MWCNT) may be explored as promising electrode material in next generation supercapacitors.

Introduction

Over the past decades, energy storage systems are the need of hour due to its significant utilization by the consumers in their daily life that includes portable electronic gadgets and electrified vehicles. And of course, rapid consumption of conventional energy sources and world's population enhancement rate led to the initiative step for the development of alternate energy source with nice qualities (low cost, highly efficient and environment benign) [1-3]. Furthermore, it has prophesied that the energy consumption by the human community has been increased thrice by 2040. Certainly, supercapacitors (SCs) are the better candidates that expected to produce sustainable electric power continuously over the conventional energy systems [4].

SCs are the hot topic of the energy world that demonstrates its potential by superior power capabilities, long cycle life and so on. Generally, SC is made up of two electrodes (say cathode and anode) which are separated by electrolyte (whether it may be aqueous or organic) and separator (for transfer of ions from the electrode). Further, it could be classified into two major categories depending upon the charge storage mechanism. They are (i) electric double layer capacitor (EDLC, conventional capacitor) and (ii) pseudocapacitor. Carbon-based electrodes (graphene, carbon nanotubes, activated carbon, carbon derived from natural source) [5-7] possess porous structure (mesopores, micropores and macropores) that probably provides more active sites in the electrode/electrolyte interfaces thereby enhances the electrochemical activity. The reaction kinetics of the EDLC electrodes is limited by the surface area which is accessible to the electrolyte ions. Transition metal oxides/hydroxides/sulfides and conducting polymers [8-10] are served as prominent electrodes in pseudocapacitors that utilizes fast Faradic reversible reactions to harvest energy. But, low electronic conductivity and poor cycle life (crystal shrinkage at long-term cycles) retards their usefulness in commercialization.

Recently, transition metal sulfide family (NiS_x, Co_xS_y, Mn_xS_y and V_xS_y) has governed more attention among the research domain on account of their superior qualities such as multiple redox states, layered structure, easy to synthesis in any anticipate architectures, high theoretical capacity and so on [11]. Unambiguously, Co_xS_y are the emerging species have received considerable interest among the SC community

* Corresponding author.
E-mail address: rathinamala@vvvcollege.org (I. Rathinamala).

https://doi.org/10.1016/j.est.2020.102200
Received 25 October 2020; Received in revised form 16 December 2020; Accepted 17 December 2020
Available online 26 December 2020
2352-152X/

owing to their salient features like high theoretical capacitance (almost 3000 F g^{-1}), attractive crystal structures (CoS, CoS_2, Co_3S_4, Co_4S_3 and Co_9S_8), good physicochemical properties, low cost and eco-friendly nature [12-15].

For instance, Amaresh and his research [16] team followed microwave mediated synthesis for the preparation of CoS_2 nanoparticles and study their applications in supercapacitors. An asymmetric supercapacitor based on Co_9S_8 nanostructures were fabricated by Mao and his labmates [17] and it could deliver a power density of 1.1 kW kg^{-1}. However, poor electronic conductivity and mechanical instability in Co_xS_y regime hinders its practical usage as electrode in SC. This could be resolved by a facile strategy, i.e hybrid supercapacitor, hybridization of carbonaceous material with cobalt sulfide matrix. The hybridization phenomenon united the advantages of both EDLC and pseudocapacitive electrode. Moreover, it restricts the set-back evolved in SCs. Among the carbon family, multi-walled carbon nanotubes has placed its footprints as landmark in various applications due their excellent properties that includes high electronic conductivity (10^8 S m^{-1}), good chemical stability, porous network structure, large specific surface area (1500 m^2 g^{-1}) and so on [18]. For instance, randomly oriented multi-walled carbon nanotube [19] could deliver a specific capacitance of 135 F g^{-1}. A maximum specific capacitance of 180 F g^{-1} was obtained by single walled carbon nanotube electrodes with excellent cyclic performance [20].

As a result, transition metal sulfide-carbon nanocomposite electrodes are found to be the better choice for electrode materials in high performance supercapacitors. They provide excellent electrochemical performance and high electrical conductivity when compared with transition metal based electrodes [21-23]. Nanoparticles anchored on honeycomb like structured $MnCo_2S_4$ nanostructures were fabricated by simple chemical bath approach and studied its potential for supercapacitor applications [24]. Liu et al. [25] designed an asymmetric supercapacitor utilizing nickel cobalt sulfide nanosheet arrays and activated carbon as electrodes. The fabricated device exhibits high capacity, large energy density and extended cycle life. Chen and his research team [26] fabricated high performance asymmetric supercapacitor ($NiCo_2S_4$ nanotubes//NGF//AC) and it could capable of delivering an ultra-high energy density of 36 W h kg^{-1}. Cheng et al [27] synthesized Co_3S_4 hollow nanocages on intertwined polypyrrole tubes and it shows outstanding electrochemical activity (1706 F g^{-1} at a current density of 1 A g^{-1}) along with high rate capability (73.2 % retention at 10 A g^{-1}).

This aside, obviously, the mode synthetic approach to be handled also decides the rational design (particle morphology) which facilitates ion exchange in electrochemical process. Wide ranges of nanostructures (nanoflakes, nanosheets, nanoflower, and nanodiscs) [28-30] with large specific surface area have demonstrated their electrochemical properties even at higher current rates. Due to the practical difficulties in the synthesis part, the fabrication of cobalt sulfide matrix with unique architecture still remains a challenge for the current research. In this context, we have adopted ultra-fast microwave-oven irradiation method to fabricate Co-S/C matrix with controlled reaction kinetics (very fast manner) and porous architectures [31]. The structural, morphological and electrochemical investigations have been presented briefly in next sections. For the first time, a polypropylene (separator) based hybrid supercapacitor was fabricated via layer over layer model.

Experimental Section

Chemicals

Cobalt nitrate hexahydrate (99%, SRL, India), multi-walled carbon nanotubes (98 %, CDH, India), thiourea (99%, Merck, India), sodium dodecyl sulfate (99%, SRL, India). The chemical used in the synthetic process are of AR grade and used without further purification.

The synthesis process is of two stages:

STAGE 1: Initially, equi-amount of cobalt nitrate hexahydrate and thiourea were dissolved (using ultrasonicator for 10 min) in 30 mL triple distilled water separately. The pinkish solution (cobalt-precursor) was allowed to stir for 15 min using magnetic stirrer and the thiourea solution was added to the precursor solution in drop-wise manner (10 drops/min). It was subjected to constant stirring (@ 300 rpm) for 30 min under room temperature. Further, the anionic surfactant was prepared in the meantime (10 mL in triple distilled water) and it was added to the stirring solution at the rate of 5 drops/min. The resultant solution was allowed to stir for 2 hrs in ambient temperature. Thus, obtained solution was transferred into 100 mL pyrex container and placed inside the microwave. The solution was subjected to microwaves at a constant power of 240 W for 10 min and allowed to cool for room temperature.

STAGE 2: The multi-walled carbon nanotubes were functionalized in acid medium and it has been reported elsewhere [32]. In the intervening period, 100 mg of functionalized multi-walled carbon nanotubes were dispersed in 1000 mL of triple distilled water and allowed to ultrasonicate for 100 min. After ultrasonication, the functionalized multi-walled carbon nanotube solution was refluxed with the resultant microwave irradiated solution and the same has been stirred for next 1 hr. The solution containing precipitate was washed thrice by triple distilled water and collects the precipitate by centrifugation. Finally, the nanocomposite has been attained by dried the precipitate at 80°C in air atmosphere. Cobalt sulfide multi-walled carbon nanotube nanostructure is described as CS-MCNT in further discussions.

Characterization Techniques

The morphology of the pristine and composite architecture prepared in the present study was examined using scanning electron microscope (SEM, TESCAN VEGA-3 LMU) and high resolution transmission microscope (HRTEM, JEOL/JEM 2100). Nitrogen adsorption-desorption experiments were carried out using Micrometrics (ASAP 2020 V3.00H) systems. Also, the porous nature and the specific surface area of the composite were estimated by Brunauer Emmett Teller (BET) method. The phase and structure analysis of the sample was conducted using PANalytical XPERT–PRO X-ray diffractometer. ESCALAB Xi^+ spectrometer (200-1000 eV) has been used to record XPS spectrum.

Fabrication of Electrodes and Electrode Assessment

In all such electrochemical studies, nickel foam serves as a current collector that possess good electrical conductivity (≈350 S cm^{-1}), mechanical strength, chemical stability and flexibility. Most importantly, the current collector helps to improve the mobility of ions in the electrode material through its plenty of pathways. Former to electrode fabrication, the current collector was ultrasonically cleaned with 5 % HCl and triple distilled water. Briefly, the working electrode was prepared by coating homogenous syrup containing 85 % of CS-MCNT (active material), 10 % of activated carbon (conductivity booster) and 5 % of PTFE (polytetrafluro ethylene, binder) over a porous pre-cleaned nickel foam (1 × 1 cm^2). The electrode was dried at 80°C for 6 hrs in air atmosphere. The typical mass loading of the electrode is 1 mg cm^{-2}. The specific capacitance, specific energy and power of the Co based composite electrodes were evaluated using the relations which are discussed in previous reports [28]. Electrochemical studies of the fabricated electrodes were performed using CH 660 D electrochemical workstation (CH Instruments, USA) in conventional three-electrode setup involving working electrode, reference electrode (Ag/AgCl- 500 μm radius) and counter electrode (Pt wire). 2 M KOH aqueous solution was served as an electrolyte. All the electrochemical characterizations (cyclic voltammetry, galvanostatic charge discharge, ac-impedance measurements) were carried out in room temperature to evaluate the supercapacitive performance of the prepared electrodes.

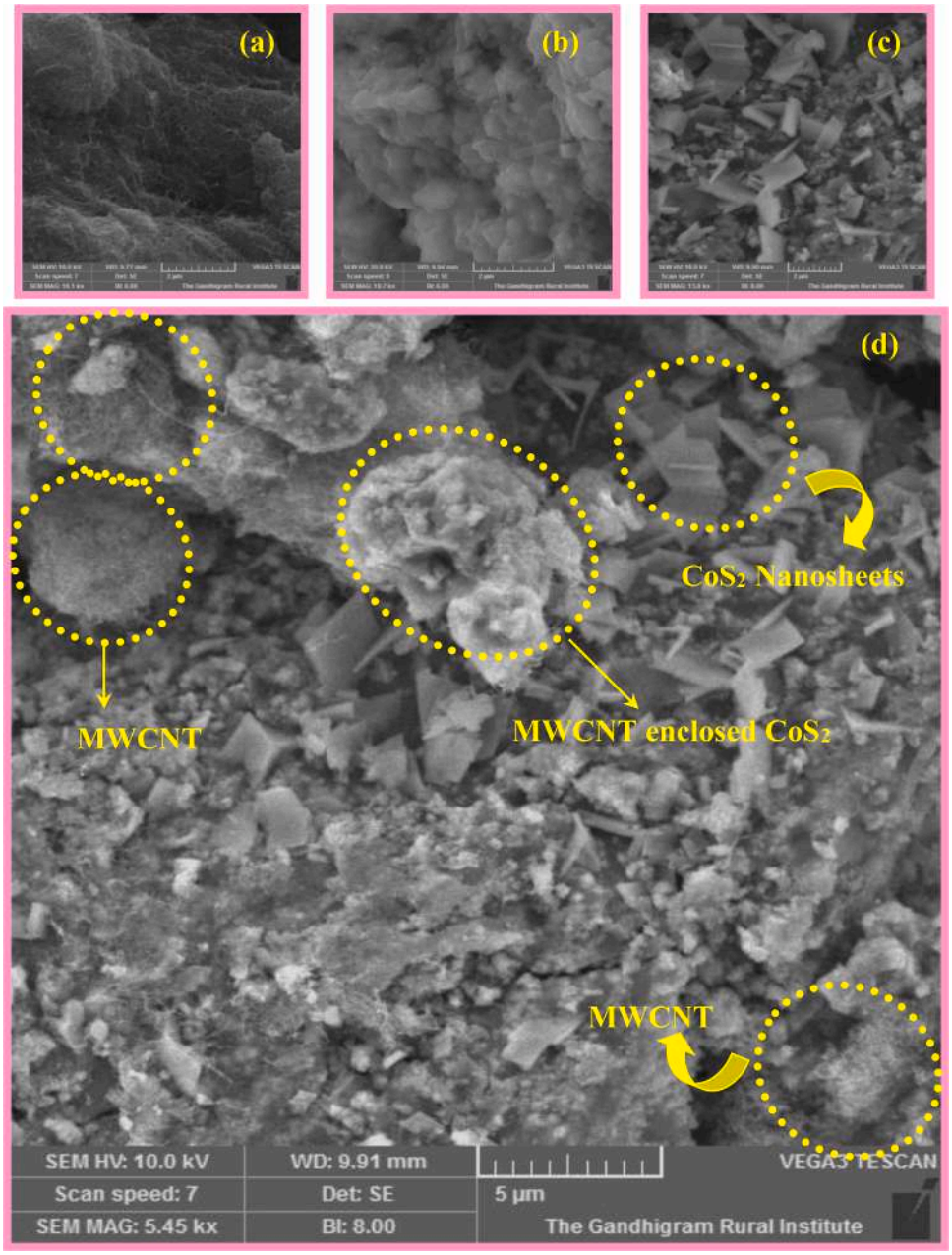

Fig. 1. Scanning electron microscope images of (a) MWCNT; (b) Pristine CoS_2; (c, d) CoS_2/MWCNT nanocomposite under various magnifications

Assembly of Hybrid Supercapacitor

The sandwich prototype hybrid supercapacitor was fabricated utilizing CS-MCNT as one electrode and functionalized multi-walled carbon nanotube as other electrode. A thin polypropylene sheet has been used as separator and the same was soaked in 6 M KOH (as electrolyte) overnight before processing. The electrochemical investigations were carried out in room temperature. Based on the mass coated on the electrodes (mass-balance theory) [33], the specific capacitance, specific energy and power of the fabricated device was calculated.

Result and Discussion

Morphological, Elemental Structural and Textural Investigations

The scanning electron microscopic images of the samples were produced in the panels of the Fig. 1. The micrometric scale of functionalized multi-walled carbon nanotubes (Fig. 1a) clearly reveals the even distribution of nanotubes having the tube width of 20-25 nm.

Regularly arranged dense sheet like morphology has been observed from the pristine cobalt sulfide (Fig. 1b). Added to that, it is interesting to mention that the sheets are laid on over other which seems to ease pathway for the ion intercalation [34] and the average thickness of the sheet was found to be ~ 250 nm. Fig. 1 (c, d), shows the representative SEM images of cobalt sulfide/multi-walled carbon nanotube composite, indicating that the carbon tubes were scattered as well as dispersed over cobalt sulfide in random manner. Moreover, presence of numerous voids in the composite leading to the opening of porous network that arrangement probably favours for enhanced electrochemical reactions. Also, some of the sheets were loosely bounded to the composite which is due to the weak Vander Waals force of attraction between the precursors leading to the collapse of sheets from the bundle [28].

The presence of elements in the nanocomposite has been identified through energy dispersive spectroscopy (EDS). The EDS spectrum

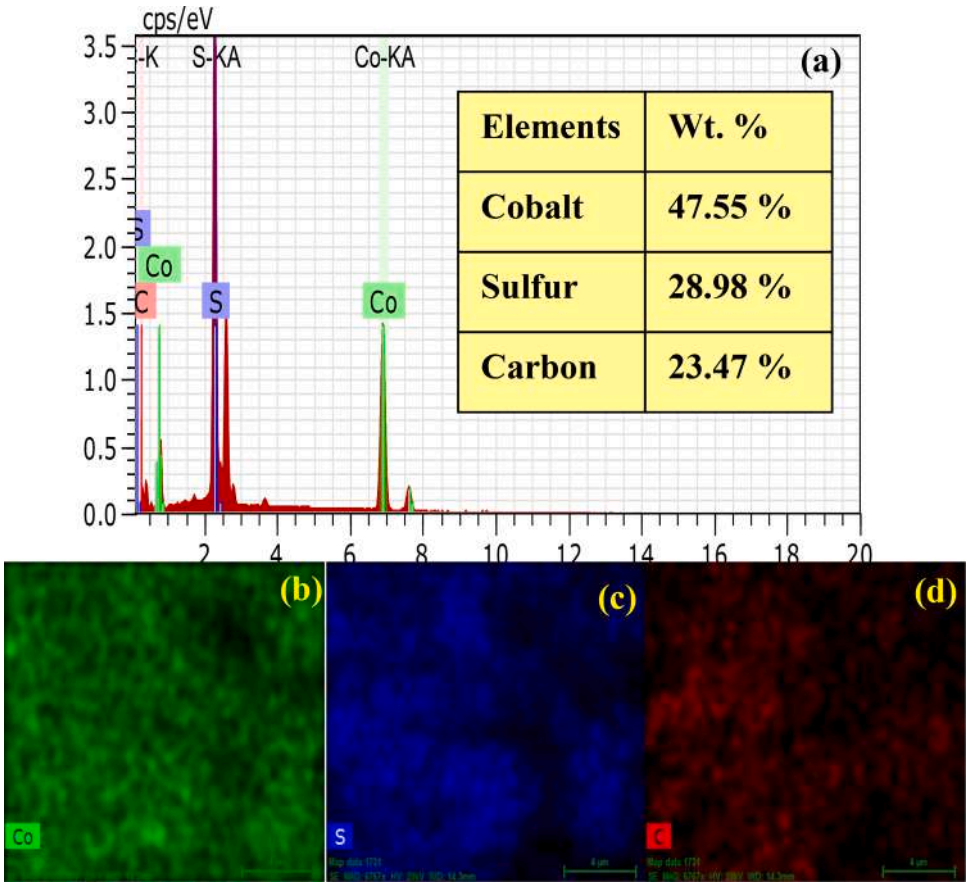

Fig. 2. (a) Energy dispersive spectrum of the prepared nanocomposite; (b-d) Elemental mapping images of cobalt, sulfur and carbon

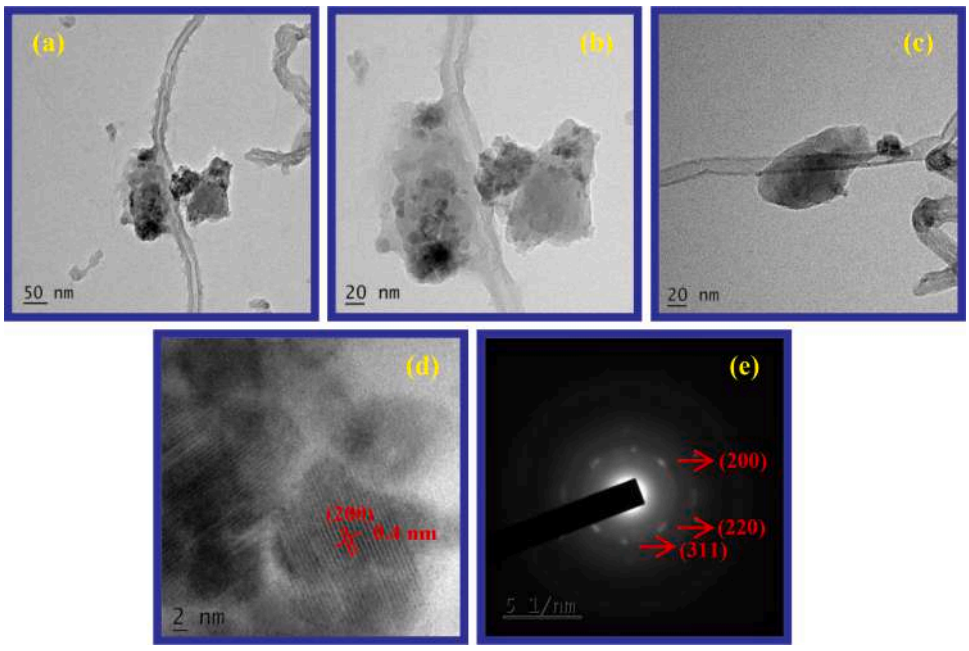

Fig. 3. (a-d) HR-TEM images of the prepared nanocomposite; (e) Corresponding SAED pattern

(Fig. 2a) confirms the presence of cobalt, sulfur & carbon in the nanocomposite and the inset shows the atomic weight percentage of the individual constituents. It is noteworthy to mention that; the occurrence of two peaks for the cobalt in the EDS spectrum suggesting the secondary peaks of cobalt (corresponds to $Co2p_{3/2}$ & $Co2p_{1/2}$). The chemical composition, valence states and oxidation states of the elements present in the prepared composite were further diagnosed through XPS analysis and their corresponding findings were presented in supporting information (Fig. S1). The high resolution XPS spectrum of Co2p shows two major peaks around 782 eV and 797 eV with the energy gap of 15 eV and

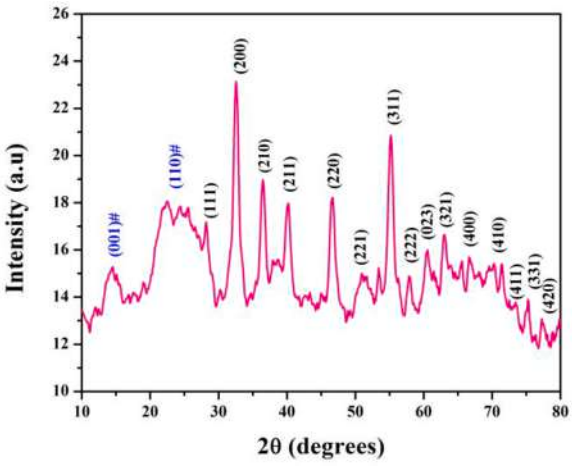

Fig. 4. XRD pattern of cobalt sulfide/MWCNT nanocomposite

it was well agrees with standard values [35,36]. The obtained peaks were ascribed to the characteristic shakeup satellites of cobalt (+2 & +3). An intense peak located at 303 eV attributed to the presence of carbon family which was slightly shifted due to the excess sulfur in the parent matrix [37]. Also, a strong peak originated at 168 eV confirms the presence of sulfur in the nanocomposite [38].

Addition to that, the homogeneity of the elements in the prepared composite has been confirmed by elemental mapping analysis (Fig. 2b-d). Further, the morphology of the prepared products was intensely analyzed using high resolution transmission electron microscope. In which (Fig. 3a-d), the carbon nanotube is firmly attached to the Co-S matrix. From the HR-TEM images, it was evident that a sheet like morphology was the basic building bricks of the nanocomposite. Fig. 3e represents the SAED pattern of CS-CNT, indicating the presence of diffused dark rings with bright spots. The bright spots in the SAED pattern suggesting the transition salts which corresponds to diffraction planes. In line with SEM studies, the high resolution micrographs confirm the morphology of the prepared nanocomposite. TEM mapping analysis was recorded for the prepared nanocomposite to support the EDS claim. TEM mapping images confirm the presence and homogeneity of Co, S and C in the prepared nanocomposite and the same have been provided in the supporting information (Fig. S2).

In order to analyze the structural parameters and diffraction planes of the prepared sample, XRD analysis was made (2θ: 20° to 80°). The major peaks (Fig. 4) located at 2θ: 32.72°, 36.63°, 40.09°, 46.58° and 55.01° were indexed to the diffraction planes of (200), (210), (211), (220) and (311) respectively. The observed major diffraction planes were well coincides with the (standard JCPDS File No: 89-3056) [39-42] cubic structured CoS_2 with the space group of Pa3. Addition to that, some other peaks located at 14.21° and 24.16° would corresponds to the graphitic carbon which is achieved from multi-walled carbon nanotube. The ratio of the two products (CoS_2 and MWCNT) has been estimated using the relative maximum peak intensity relations [43,44] and it was found to be 0.5622 and 0.4377. Also, the average crystallite size has been estimated using the De-Bye Scherrer relation and it was found to be 18.04 nm.

Formation Mechanism of CS-MCNT Nanocomposite

Scheme 1, illustrates the possible pictorial representation for the formation mechanism of the cobalt sulfide/multi-walled carbon nanotube composite. Initially, C=S bond in the thiourea has been broken by the oxygen species (present in the water molecules) with the liberation of hydrogen sulfide [45]. The excess of H_2S released in the process reacts with the Co^{2+} precursors and started homogeneous nucleation. The nucleation process gets wind up after the formation of small crystalline CoS_x nuclei. As the time rolled, several tiny nuclei were formed and initiated the growth mechanism due to the low surface energy. After being the nucleus was irradiated by microwaves, the growth of the particles along one particular (Ostwald's ripening phenomena) direction and leads to the formation of two dimensional sheet-like morphology. Next, the highly active and adhesive (surface has been etched in acid medium) functionalized multi-walled carbon nanotubes were refluxed with these sheets. Due to the low Vander Walls force between the sheets and carbon nanotubes, they bind together results in opening of numerous pathways for ion insertion/re-insertion that probably enhances the electrochemical phenomenon.

Textural Features of CS-MCNT

From the morphological observations, it was identified that the surface of the prepared composite was enriched with several pores and it was further confirmed through nitrogen adsorption/desorption

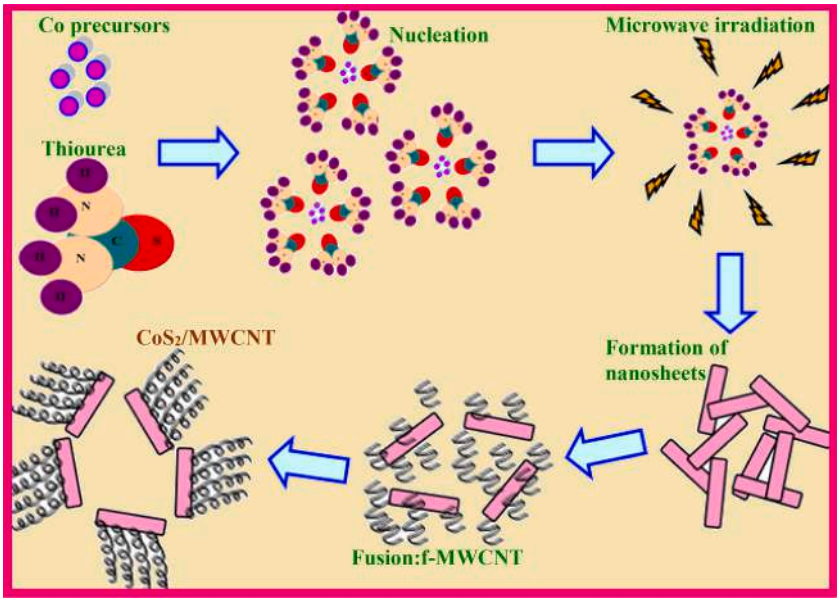

Scheme 1. Pictorial representation for the formation of CoS_2/MWCNT nanocomposite

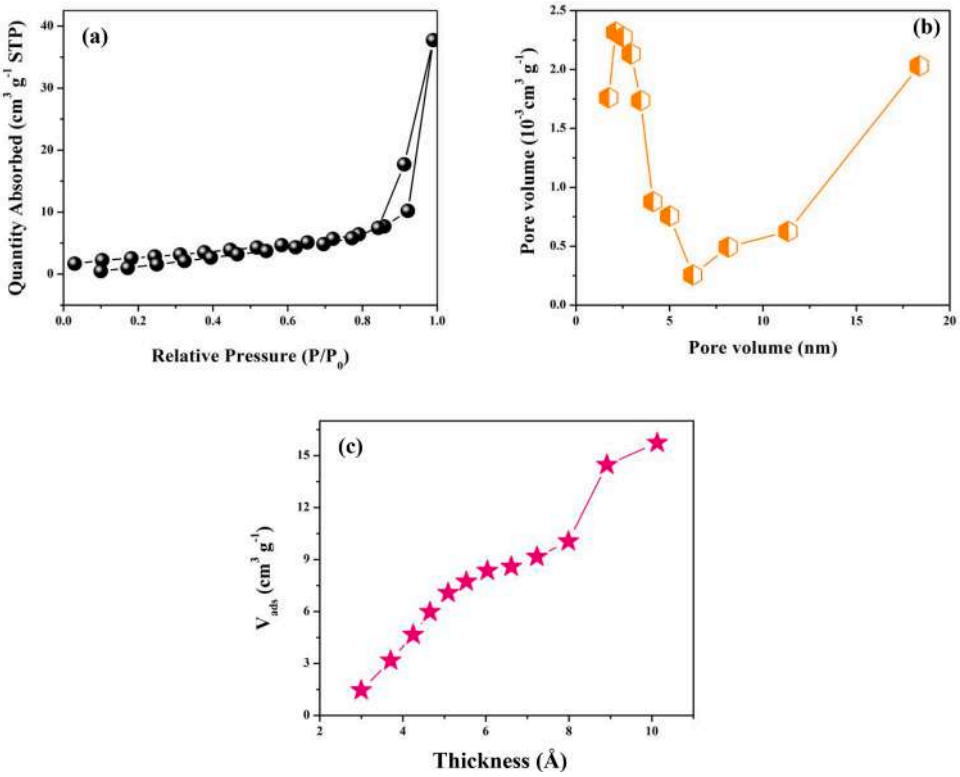

Fig. 5. (a) Nitrogen adsorption/desorption isotherms of CoS_2/MWCNT nanocomposite; (b) Pore size distribution profile; (c) t-plot

experiments. The textural features associated with CS-MCNT nanocomposite was produced in the panels of Fig. 5. The nitrogen adsorption/desorption plot (Fig. 5a) shows a hysteresis loop ranging from 0 to 1.0 (P/P_0), indicating the typical type IV isotherms.

The specific surface area and total pore volume of the sample has been estimated using BET method and it was found to be 15.735 $m^2\ g^{-1}$ and 0.063 $cm^3\ g^{-1}$. Also the pore distribution profile is depicted in Fig. 5b, confirms the presence of mesopores [46]. (Pores lie within the range from 2 nm to 20 nm). Furthermore, De-Bore's t-plot was engaged to study the presence of micropores in the prepared composite. It consists of two linear segments with slight deviation (at 0.7 nm) which is due to the complete filling of micropores. The t-plot (Fig. 5c) shows the total pore volume of and 0.0238 $cm^3\ g^{-1}$ with the external surface area of 9.674 $m^2\ g^{-1}$. The presence of mesopores in the sample provides the efficient route electrolyte ions.

Supercapacitive Property of CS-MCNT Electrode

The cyclic potential response for CS-MCNT electrode at various sweep rates (2-50 mV s^{-1}) in an alkaline medium is presented in Fig. 6a, displays a pair of symmetric redox peaks. This indicates the charge storage process is accomplished by Faradic redox phenomenon. The chief electrochemical reaction involved in the parent matrix is expressed as follows[47]:

$$CoS_2 + OH^- \leftrightarrow CoS_2OH \quad (1)$$

$$CoS_2OH^- \leftrightarrow CoS_2O \quad (2)$$

The specific capacitance of the prepared electrode has been estimated and it was found to be 524 F g^{-1} (Fig. 6a inset), is 30 % higher than the pristine electrodes. It is noteworthy to mention that, the specific capacitance of the electrode decreases while increasing the scan rates. A unanimous truth behind the fact is the incomplete access of the electrolyte ions at the outer surface of the electrode material [48]. Also, a comparison profile (@ 2 mV s^{-1}) is shown in Fig. 6b, indicating higher area of CS-MCNT electrode than the pristine cobalt sulfide results in better electrochemical process. Since, the fabricated electrode is composed of CoS_2 and MWCNT, it is very mandatory to identify the Faradic and non-Faradic capacitance in the total capacitance. It was estimated using the following equation,

$$i(v) = k_1 v + k_2 v^{1/2} \quad (3)$$

The total current developed in the CV plot is the sum of capacitive process and ion diffusive process. It is evident that, (Dunn's method [28] depicted in Fig. 6c) the total specific capacitance evolved from the composite material is the sum of the Faradic capacitance (451 F g^{-1} due to cobalt sulfide) and non-Faradic capacitance (73 F g^{-1} due to MWCNT).

The specific capacitance, rate performance and stability of the cobalt sulfide/multi-walled carbon nanotube composite electrodes were further examined by galvanostatic charge/discharge method. The charge/discharge measurement has been carried for the fabricated electrodes at different current densities in 2 M KOH solution. Fig. 6d shows the charge/discharge plateaus of CS-MCNT electrodes, indicating the non-linearity in curves. This confirms the charge storage is done by the combination of Faradic and non-Faradic electrode material. The GCD plot of CS-MWCNT, pristine cobalt sulfide and MWCNT is shown in Fig. 6e. The estimated specific capacitance values from the discharge curves were found to be 536 F g^{-1} whereas pristine cobalt sulfide and MWCNT electrodes shows a specific capacitance of 379 F g^{-1} at a specific current of 2 A g^{-1} respectively . It is noteworthy to mention that the fabricated electrode shows higher specific capacitance which is 29.2 % higher than the pristine CoS_2 and 70.1 % higher than MWCNT. The specific capacitance obtained in the present work is quite good while compared with the previously reported cobalt sulfide based carbon systems [41,49-51]. This is probably due to the presence of mesoporous sheet-like morphology which causes opening up of additional sites for the electrolyte ions. Interestingly, the specific capacitance of the electrode material decreases while raising the current densities (Fig. 6f). The common fact behind the phenomenon is the internal resistance

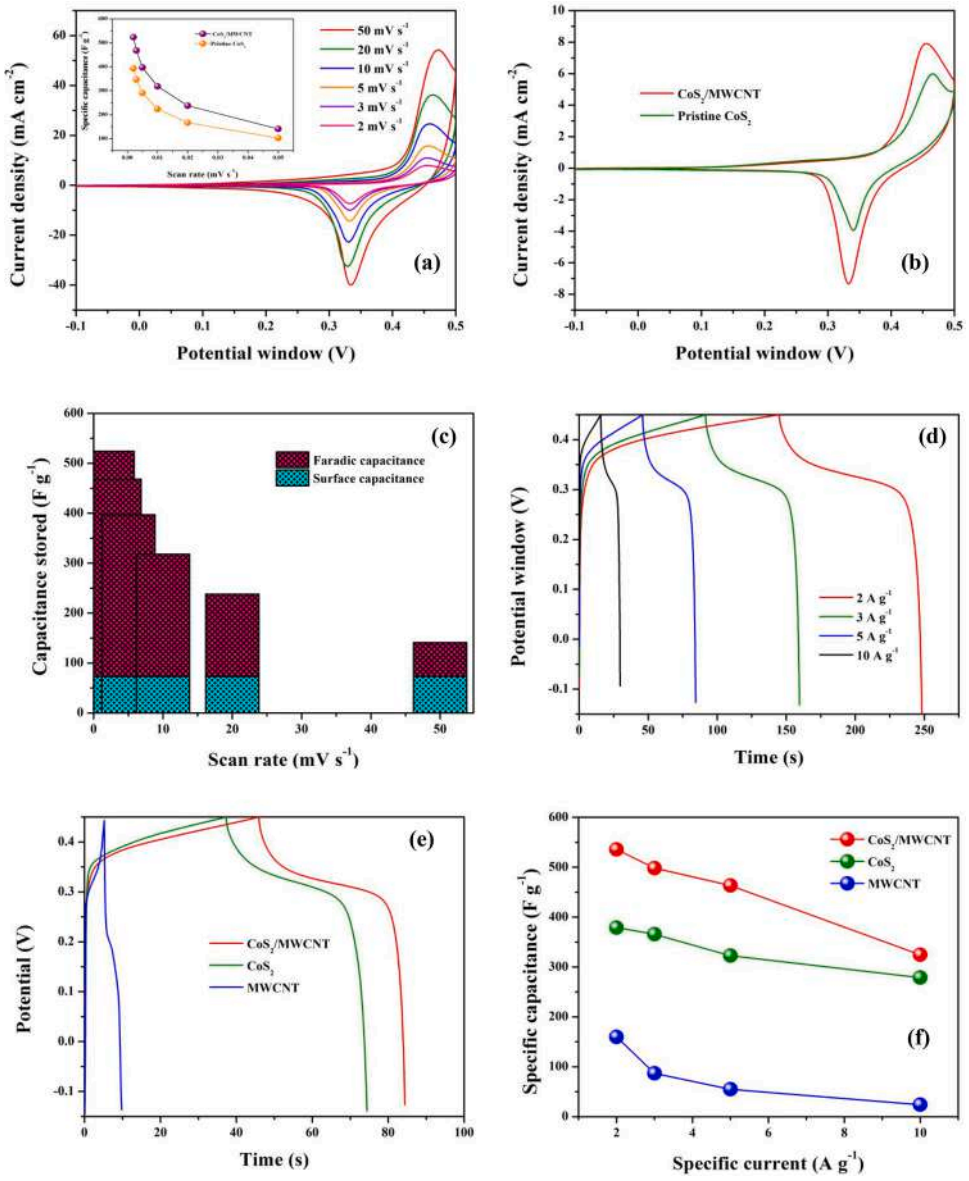

Fig. 6. (a) Cyclic voltammetric responses of the prepared nanocomposite at various scan rates (vs Ag/AgCl); (b) Comparison plot of pristine/composite at 2 mV s^{-1}; (c) Amount of capacitance stored at different potential sweep rates; (d) Galvanostatic charge/discharge plateaus of CoS_2/MWCNT nanocomposite; (e) comparison plot of pristine/composite at 5 A g^{-1}; (f) Variation of current density as a function of specific capacitance

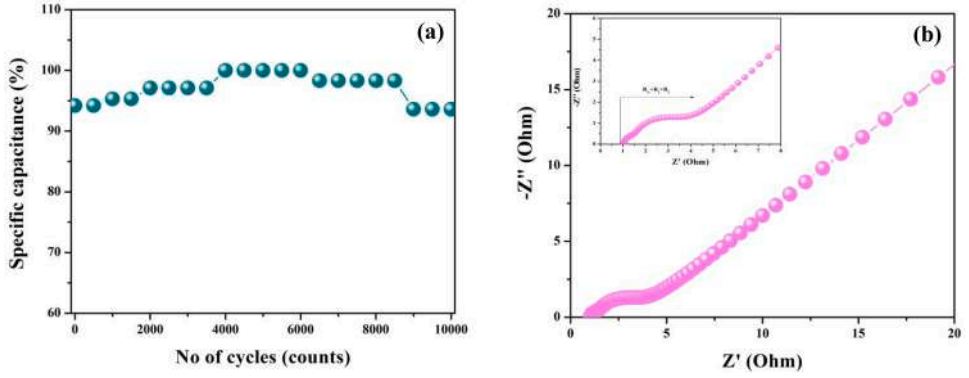

Fig. 7. (a) Cyclic life of CoS_2/MWCNT electrodes over 10000 charge/discharge cycles at a high current density of 10 A g^{-1}; (b) Impedance plot of CoS_2/MWCNT nanocomposite (inset: Magnified spectrum)

Table 1
Literature survey of cobalt sulfide/carbon based architectures

Sl.no	CoS_x/C based System	Morphology	Electrolyte	No of cycles	Capacitance Retention	Reference
1	CoS_x/MWCNT	Nanosheets	2 M KOH	1000 cycles	95 %	41
2	CoS_2-C@TCL.	Nanocages	2 M KOH	2000 cycles	88 %	47
3	CoS_2/RGO	Nanosheets	6 M KOH	2000 cycles	97 %	49
4	CoS_2-Graphene	Nanosheets	6 M KOH	1000 cycles	99 %	50
5	PANI/RGO/CoS	Nanosheets	1 M H_2SO_4	1000 cycles	90.1 %	51
6	Carbon coated Co_9S_8	Nanoflower	2 M KOH	10000 cycles	86 %	52
7	CoS_2/RGO	Nanosheets	6 M KOH	2000 cycles	95.4 %	53
8	CoS/CNT	Nanoparticles	6 M KOH	1000 cycles	93.4 %	54
9	CNTs/Co_3S_4	Nanosheets	1M of $NaClO_4$	100 cycles	82.89 %	55
10	rGO-Co_3S_4	Nanosheets	1MH_2SO_4	5000 cycles	81.7 %	56
11	CS-MWCNT	Nanoflakes	2 M KOH	10000 cycles	93.6 %	Present work

Table 2
Device performance of cobalt sulfide/carbon based supercapacitors

Sl. no	CoS_x/C based System	C_s F g^{-1}	Specific Energy (W h kg^{-1})	Specific Power (W kg^{-1})	Electrolyte	No of cycles	Capacitance Retention	Reference
1	Ni-Co-S/NF//AC/NF	61.8	24.8	849.5	1 M KOH	1000	88.6 %	21
2	CoS/RGO//AC	36.5	13.8	824.6	6 M KOH	2000	95.4 %	53
3	CoS_x-NSA//RGO	47	14.68	369	1 M Na_2SO_4	3000	84 %	59
4	Co_3S_4//Co_3S_4-rGO	164 mF cm^{-2}	1.09	398	2 M KOH	5000	89.56 %	60
5	CoS/graphene//AC	–	29	800	2 M KOH	10000	70 %	61
6	2D Co_9S_8 //AC	82.9	31.4	200	3 M KOH	5000	90 %	62
7	CS-MWCNT//MWCNT	56	8.16	696	6 M KOH	5000	83.8 %	Present Study

developed within the electrode material [28]. Further, the cyclic life test was executed for the fabricated electrodes to identify the suitability of the electrode material in supercapacitor domain. Stability test was carried out (10, 000 continuous charge/discharge cycles) at a possible specific current of 10 A g^{-1} in an alkaline medium. The stability profile of CS-MCNT electrode is provided in the Fig. 7a. For the first 2000 cycles, a gradual rise in capacitance which is attributed to the activation of the electrode material and it also rises progressively for the next 4000 cycles. After that, the specific capacitance of the electrode material started to decay indicating the closing of active channels in the electrode surface. The insertion and de-insertion of the electrolyte ions into electroactive species thereby creates a mechanical stress that leads to decrease in capacity [34]. Finally, the electrode exhibits 93.6 % capacitance retention at the end of 10, 000 continuous charge/discharge cycles. This could be attributed to the facile morphology of the prepared nanocomposite which withstands even at continuous cycling process. The morphology and crystallinity of the nanostructures was studied after cycling process and the results are provided in the supporting information (Fig. S3). Also, the morphology of the nanostructure gets slightly altered at the end of cyclic process. The cycle life of CS-MCNT electrode is fairly higher than the previously reported works [41,47, 49-56] and they are presented in the table T1. The stability profile of pristine cobalt sulfide is presented in supporting information (Fig. S4). Further, the Coulombic efficiency of the prepared electrodes was estimated using the relation which is reported elsewhere [57]. The electrode shows 96 % Coulombic efficiency (Fig. S5) at the end of 10, 000 charge/discharge cycles. Fig. 7b, shows the impedance spectrum of cobalt sulfide/carbon composite prepared in the present study. The thus-obtained spectrum was fitted to the equivalent circuit, which is composed of several components discussed briefly in our previous work [58]. The plot consists of two semi-circle regions corresponding to the Faradic process occurred in electrode material (Faradic and non-Faradic material) and a linear platform which is attributed to the diffusion controlled process. The charge transfer resistance of the electrode material was estimated by extending the semi-circle region and it was found to be 2.1 Ω (1.0 Ω for CoS_2 +1.1 Ω for MWCNT). A possible least charge transfer resistance developed in the electrode material leading to the enhanced electrochemical process. Impedance spectrum of pristine material is produced in supporting information Fig. S6).

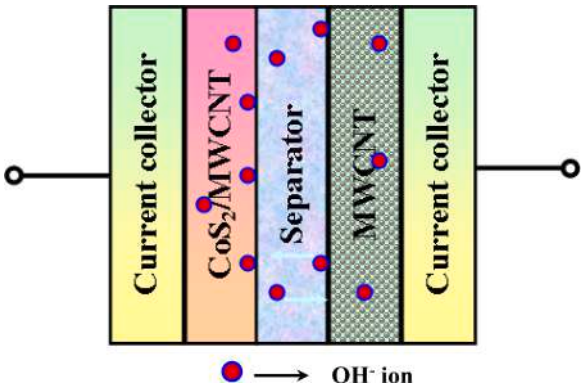

Scheme 2. Schematic representation of design of a supercapacitor

Table 1 and table 2

Device Performance (CS-MCNT//6 KOH//MWCNT)

To extend the potential features of the fabricated electrodes (CS-MCNT), we have devised to design the hybrid supercapacitor based on multi-walled carbon nanotubes (CS-MCNT// Polypropylene & 6 KOH// MWCNT). As discussed earlier, our primary task is to enhance the specific energy/power of the device. By extending the potential window, thereby chance of enhancing such parameters [48]. Here, we have chosen multi-walled carbon nanotube electrode as the counter electrode. The excess of ions involved in the mechanism has been tackled by the counter electrode. Also, multi-walled carbon nanotubes act as mechanical strength to the system. Based on the mass-balance theory [33], the active mass of the counter electrode has been estimated. The schematic illustration of the cobalt sulfide/multi-walled carbon nanotube

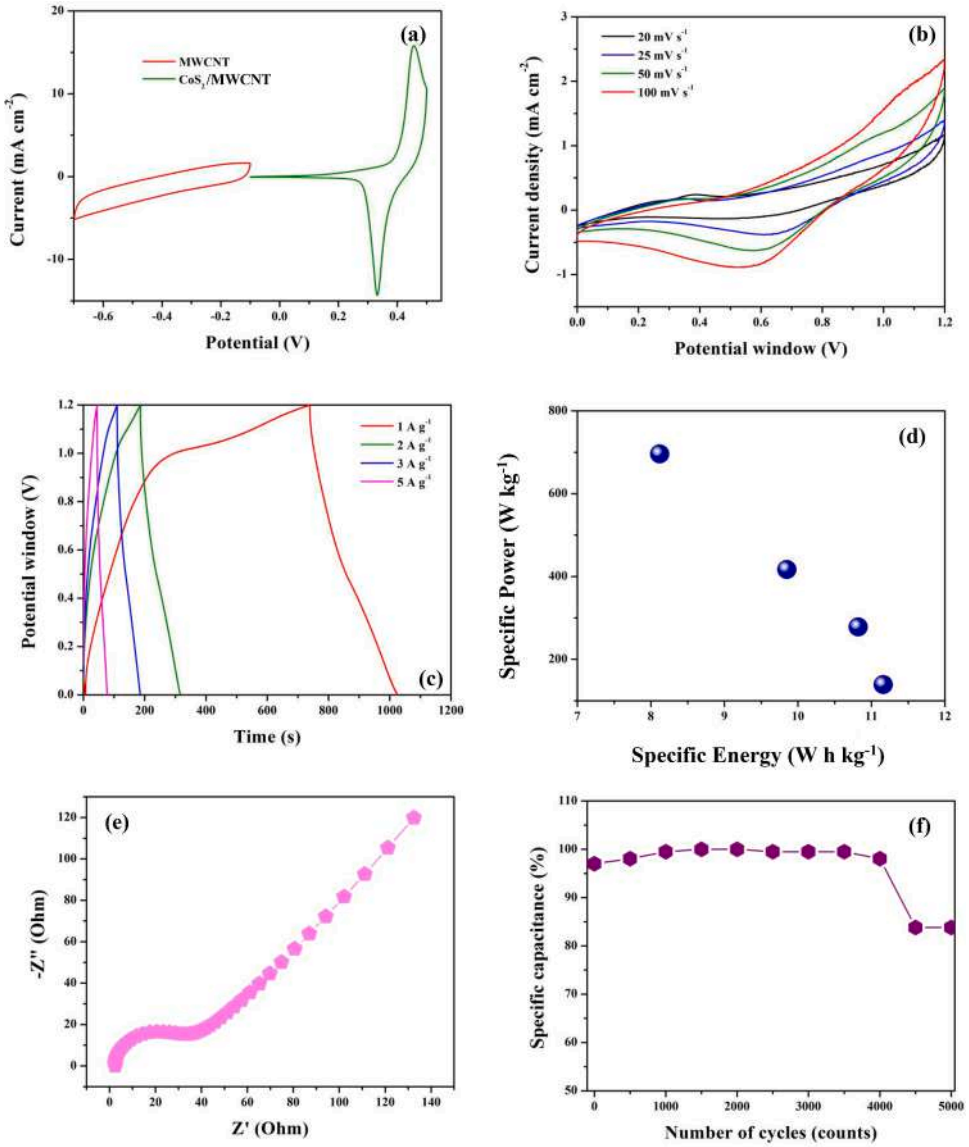

Fig. 8. (a) CV profile of MWCNT and CoS_2/MWCNT; (b) CV traces of hybrid supercapacitor; (c) Charge/discharge profile of the device; (d) Ragone plot; (e) Impedance spectrum of the hybrid cell; (f) Stability layout of two terminal mode

based hybrid supercapacitor is presented in Scheme 2.

The electrochemical responses of the hybrid device were produced in the panels of Fig. 8. Fig. 8a shows the cyclic voltammograms of the MWCNT and CS-MWCNT electrodes in aqueous alkaline solution. The CV traces (Fig. 8b) of the device (20-100 mV s^{-1}) portrays the charge storage mechanism is completed by Faradic redox process. Also, the area of the CV curve enhances while increasing the potential. Further, the specific capacitance of the cell was estimated through galvanostatic charge-discharge method (Fig. 8c). In which, different current densities were applied to the electrodes at constant window. It exhibits the plateaus that resemble both Faradic and double layer nature of charge storage.

Moreover, the specific capacitance of the hybrid cell was calculated and it was found to be 56 F g^{-1}at a current density of 1 A g^{-1}. The Coulombic efficiency of fabricated device is 39 %, 76%, 71% and 74% at a specific current of 1 A g^{-1}, 2 A g^{-1}, 3 A g^{-1} and 5 A g^{-1}. However, the Coulombic efficiency at lower current (1 A g^{-1}) is quite low which is attributed to the irreversibility of Nernstain phenomenon [57]. Since, the fabricated cell was polarized upto + 1.2 V (to prevent the hydrogen and oxygen evolution) it hinders the energy density of the two terminal system [48]. The specific energy and power of the hybrid device was estimated based on the mass loaded on the device (Fig. 8d). It provides a high specific energy of 8.16 W h kg^{-1} with the ultra- high specific power of 696 W kg^{-1}.

The resistive elements indulging the capacitive properties were identified using a.c. impedance measurements (Fig. 8e). The obtained data was fitted to the equivalent model and it shows the charge transfer resistance of 35.5 Ω. A long-term cyclic process (5000 cycles at a practical current density of 10 A g^{-1}) was carried out to identify the stability of the hybrid supercapacitor (Fig. 8f). At the final stage, the device shows 83.8% of capacitance retention.

A comparison profile for the electrochemical responses of the previous reported CoS_x/C based hybrid supercapacitor has been provided in the table T2 [21,53,59–62]. Such enduring qualitative merits associated with the device make them a better candidate in future energy storage systems.

Conclusion

In conclusion, we have successfully synthesized CoS_2/multi-walled carbon nanotube architecture using structure directing agent. The structural, morphological, textural and electrochemical investigations

have been made on the prepared electrodes in order to study the supercapacitive properties. Cyclicvoltammetry analysis reveals that CS-MCNT electrodes exhibit pseudocapacitive nature and capable of delivering the specific capacitance of 524 F g^{-1}. Morphological studies portray the formation of interconnected sheet-like architecture with porous network. A very low charge transfer resistance of 2.1 Ω was estimated from EIS makes enhanced electrochemical performance. Moreover, a hybrid asymmetric supercapacitor has been fabricated and it could capable of delivering an ultra-high specific power of 696 W kg^{-1}. The results arrived from the CS-MCNT electrode suggesting a promising electrode material in next-generation supercapacitors.

Declaration of Competing Interest

The authors declare that they have no conflict of interest.

Supplementary materials

Supplementary material associated with this article can be found, in the online version, at doi:10.1016/j.est.2020.102200.

References

[1] B. Xie, M. Yu, L. Lu, H. Feng, Y. Yang, Y. Chen, H. Cui, R. Xiao, J. Liu, Pseudocapacitive Co_9S_8/Graphene Electrode for High-Rate Hybrid Supercapacitors, Carbon 141 (2019) 134.

[2] Z. Jiang, W. Lu, Z. Li, K.H. Ho, Xu Li, X. Jiao, D. Chen, Synthesis of Amorphous Cobalt Sulfide Polyhedral Nanocages for High Performance Supercapacitors, J. Mater. Chem. A 2 (2014) 8603.

[3] S. Zheng, X. Li., B. Yan, Q. Hu, Y. Xu, X. Xiao, H. Xue, H. Pang, Transition-Metal (Fe, Co, Ni) Based Metal-Organic Frameworks for Electrochemical Energy Storage, Adv. Energy Mater. (2017), 1602733.

[4] Y. Ruan, L. Lv, Z. Li, C. Wang, J. Jiang, Ni Nanoparticles @ Ni-Mo Nitride Nanorod Arrays: A Novel 3D-Network Hierarchical Structure for High Areal Capacitance Hybrid Supercapacitors, Nanoscale 9 (2017) 18032.

[5] F. Yi, H. Ren, J. Shan, X. Sun, D. Wei, Z. Liu, Wearable Energy Sources Based on 2D Materials, Chem Soc Rev 47 (2018) 3152.

[6] F. Wang, X. Wu, X. Yuan, Z. Liu, Y. Zhang, L. Fu, Y. Zhu, Q. Zhou, Y. Wu, W. Huang, Latest Advances in Supercapacitors: From New Electrode Materials to Novel Device Designs, Chem Soc Rev 46 (2017) 6816.

[7] D.P. Dupal, N.R. Chodankar, D.H. Kim, P.G. Romero, Towards Flexible Solid – State Supercapacitors for Smart and Wearable Electronics, Chem Soc Rev 47 (2018) 2065.

[8] K. Xiang, Z. Xu, T. Qu, Z. Tian, Y. Zhang, Y. Wang, M. Xie, X. Guo, W. Ding, X. Guo, Two Dimensional Oxygen-Vacancy-Rich Co_3O_4 Nanosheets with Excellent Supercapacitor Performances, Chem Comm 53 (2017) 12410.

[9] J. Azadmanjiri, V.K. Srivastava, P. Kumar, M. Nikzad, J. Wang, A. Yu, Two-and Three-Dimensional Graphene-Based Hybrid Composites for Advanced Energy Storage and Conversion Devices, J. Mater. Chem. A 6 (2018) 702.

[10] S.L. Rubaye, R. Rajagopalan, X. Dou, Z. Cheng, Facile Synthesis of Reduced Graphene Oxide Wrapped Porous $NiCo_2O_4$ Composite with Superior Performance as an Electrode Material for Supercapacitors, J. Mater. Chem. A 5 (2017) 18989.

[11] Z. Yu, L. Tetard, L. Zhai, J. Thomas, Supercapacitor Electrode Materials: Nanostructures from 0 to 3 Dimensions, Energy Environ. Sci. 8 (2015) 702.

[12] M. Yi, C. Zhang, C. Cao, C. Xu, B. Sa, D. Cai, H. Zhan, MOF-Derived Hybrid Hollow Submicrospheres of Nitrogen-Doped Carbon-Encapsulated Bimetallic Ni-Co-S Nanoparticles for Supercapacitors and Lithium Ion Batteries, Inorg. Chem. 58 (2019) 3916.

[13] S. Kandula, K.R. Shrestha, G. Raeshkhanna, N.H. Kim, J.H. Lee, Kirkendall Growth and Ostwald Ripening Induced Hierarchical Morphology of Ni-Co LDH/$MMoS_x$ (M= Co, Ni, Zn) Heterostructures as Advanced Electrode Materials for Asymmetric Solid-State Supercapacitors, ACS Appl. Mater. Interfaces 11 (2019) 11555.

[14] Y. Zhao, Z. Shi, T. Lin, L. Suo, C. Wang, J. Luo, Brownian-Snow Ball-Mechanism-Induced Hierarchical Cobalt Sulfide for Supercapacitors, J. Power Sources 412 (2019) 321.

[15] Y. Liu, S. Guo, W. Zhang, W. Kong, Z. Wang, W. Yan, H. Fan, X. Hao, G. Guan, Three-Dimensional Interconnected Cobalt Sulfide Foam: Controllable Synthesis and Application in Supercapacitor, Electrochim. Acta 317 (2019) 551.

[16] S. Amaresh, K. Karthikeyan, L.C. Jang, Y.S. Lee, Single-Step Microwave Mediated Synthesis of the CoS_2 Anode Material for High Rate Hybrid Supercapacitors, J. Mater. Chem. A 2 (2014) 11099.

[17] X. Mao, Z. Wang, W. Kong, W. Wang, Nickel Foam Supported Hierarchical Co_9S_8 Nanostructures for Asymmetric Supercapacitors, New J. Chem. 41 (2017) 1142.

[18] A.B. Dalton, S. Collins, E. Munoz, J.M. Razal, H.V. Erbron, J.P. Ferraris, J. N. Coleman, B.G. Kim, R.H. Baughman, Super-Tough Carbon-Nanotube Fibres, Nature 423 (2003) 703.

[19] N. Choudhary, C. Li, J. Moore, N. Nagaiah, L. Zhai, Y. Jung, J. Thomas, Asymmetric Supercapacitor Electrodes and Devices, Adv. Mater. 29 (2017), 1605336.

[20] K.H. An, W.S. Kim, Y.S. Park, J.M. Moon, D.J. Bae, S.C. Lim, Y.S. Lee, Y.H. Lee, Electrochemical Properties of High-Power Supercapacitors Using Single-Walled Carbon Nanotube Electrodes, Adv. Funct. Mater. 11 (2001) 387.

[21] K. Tao, X. Han, Q. Ma, L. Han., A Metal-Organic Framework Derived Hierarchical Nickel-Cobalt Sulfide Nanosheet Array on Ni Foam with Enhanced Electrochemical Performance for Supercapacitors, Dalton Trans 47 (2018) 3496–3502.

[22] K. Tao, X. Han, Q. Cheng, Y. Yang, Z. Yang, Q. Ma, L. Han, A Zinc Cobalt Sulfide Nanosheet Array Derived From 2D Bimetallic Metal-Organic Frameworks for High-Performance Supercapacitors, Chemistry- A European Journal 24 (2018) 12584–12591.

[23] X. Han, K. Tao, D. Wang, L. Han, Design of a Porous Cobalt Sulfide Nanosheet Array on Ni Foam From Zeolitic Imidazolate Frameworks as an Advanced Electrode for Supercapacitors, Nanoscale 10 (2018) 2735–2741.

[24] K.V.G. Rahavendra, C.V.V.M. Gopi, R. Vinodh, S.S. Rao, I.M. Obaidat, H.J Kim, Facile Synthesis of Nanoparticles Anchored on Honeycomb-Like $MnCo_2S_4$ Nanostructures as a Binder-Free Electroactive Material for Supercapacitors, J. *Energy Storage* 27 (2020) 101159–101166.

[25] T. Liu, J. Liu, L. Zhang, B. Cheng, J. Yu, Construction of Nickel Cobalt Sulfide Nanosheet Arrays on Carbon Cloth for Performance-Enhanced Supercapacitor, J. Mater. Sci. Technol. 47 (2020) 113–121.

[26] Y. Chen, T. Liu, L. Zhang, J. Yu, $NiCo_2S_4$ Nanotubes Anchored 3D Nitrogen-Doped Graphene Framework as Electrode Material with Enhanced Performance for Asymmetric Supercapacitors, ACS Sustain. Chem. Eng. 7 (2019) 11157–11165.

[27] ZIF- Inlaying, Derived Co_3S_4 Hollow Nanocages on Intertwined Polypyrrole Tubes Conductive Networks for High-Performance Supercapacitors, Electrochim. Acta 341 (2020) 136042–136050.

[28] I.M. Babu, J.J. William, G. Muralidharan, Surfactant Tuned Morphology of Mesoporous β-$Co(OH)_2$/CMC Nanoflakes: A Prospective Candidate for Supercapacitors, J. Solid State Electrochem. 23 (2019) 1325.

[29] I.M. Babu, J.J. William, G. Muralidharan, Hierarchical β-$Co(OH)_2$/CoO Nanosheets: An Additive-Free Synthesis Approach for Supercapattery Applications, Ionics (2019) 25–2437.

[30] K.K. Purushothaman, I.M. Babu, B. Saravanakumar, Hierarchical Mesoporous $Co_x Ni_{1-x}$ O as Advanced Electrode Material for Hybrid Supercapacitors, Int. J. Hydrogen Energy 42 (2017) 28445.

[31] J.J. William, I.M. Babu, G. Muralidharan, Lithium Ferrite (α-$LiFe_5O_8$) Nanorod Based Battery-Type Asymmetric Supercapacitor with NiO Nanoflakes as the Counter Electrode, New J. Chem. 43 (2019) 15375.

[32] B. Saravanakumar, K.K. Purushothaman, G. Muralidharan, V_2O_5/Functionalized MWCNT Hybrid Nanocomposite: The Fabrication and its Enhanced Supercapacitive Performance, RSC Adv 4 (2014) 37437.

[33] I.M. Babu, J.J. William, G. Muralidharan, $AgCoO_2$-Co_3O_4/CMC Cloudy Architecture as High Performance Electrodes for Asymmetric Supercapacitors, ChemElectroChem 7 (2020) 535–545.

[34] B. Saravanakumar, K.K. Purushothaman, Muralidharan, Interconnected Nanoporous Network for High-Performance Supercapacitors, ACS Appl. Mater. Interfaces 4 (2012) 4484.

[35] E. Dai, J. Xu, J. Qiu, S. Liu, P. Chen, Y. Liu, Co@Carbon and Co_3O_4@Carbon Nanocomposites Derived From Single MOF for Supercapacitors, Sci. Rep. 7 (2017) 12588–12598.

[36] Y. Zou, C. Cai, C. Xiang, P. Huang, H. Chu, Z. She, F. Xu, L. Sun, H.B. Kraatz, Simple Synthesis of Core-Shell Structure of Co-Co_3O_4@Carbon-Nanotube-Incorporated Nitrogen-Doped Carbon for High-Performance Supercapacitor, Electrochim. Acta. 261 (2018) 537–547.

[37] C. Zhang, L. Wang, W. Lei, Y. Wu, C. Li, M.A. Khan, O. Ouyang, X. Jiao, H. Ye, S. Mutahir, Q. Hao, Achieving Quick Charge/Discharge Rate of 3.0 V s^{-1} by 2D Titanium Carbide (MXene) via N-Doped Carbon Intercalation, Mat. Lett. 234 (2019) 21–25.

[38] M. Fantauzzi, B. Elsener, D. Atzei, A. Rigaoldi, A. Rossi, Exploiting XPS for the Identification of Sulfides and Polysulfides, RSC Adv. 5 (2015) 75953–75963.

[39] F. Fu, Y. Chen, P. Li, J. He, Z. Wang, W. Lin, W. Zhang, Three-Dimensional CoS_2/RGO Hierarchical Architecture as Superior Capability for Lithium Ion Batteries, RSC Adv 5 (2015) 71790.

[40] H. Ning, Z. Liu, Y. Xie, H. Huang, CoS_2 Coatings for Improving Thermal Stability and Electrochemical Performance of FeS_2 Cathodes for Thermal Batteries, J. Electrochem. Soc. 165 (2018) A1725.

[41] J. Tang, J. Shen, N. Li, M. Ye, A Free Template strategy for the Synthesis of CoS_2-Reduced Graphene Oxide Nanocomposite with Enhanced Electrode Performance for Supercapacitors, Ceram. Inter. 40 (2014) 15411.

[42] L. Zhang, H.B. Wu, X.W. Lou, Unusual CoS_2 Ellipsoids with Anisotropic Tube-Like Cavities and their Application in Supercapacitors, Chem. Commun. 48 (2012) 6912.

[43] P. Thiruramanathan, A. Marikani, S. Ravi, D. Madhavan, G.S. Hikku, Fabrication of Miniatured High Bandwidth Dielectric Resonator on Patch (DRoP) Antenna Using High Dielectric $CaCu_3Ti_4O_{12}$ Nanoparticles, J. Alloys Compds. 747 (2018) 1033–1042.

[44] S.G. Fritsch, T. Lebey, M. Boulos, Durand. Dielectric Properties of $CaCu_3Ti_4O_{12}$ Based Multiphased Ceramics, J. European Ceramic Soc. 26 (2006) 1245–1257.

[45] F. Luo, J. Li, H. Yuan, D. Xiao, Rapid Synthesis of Three-Dimensional Flower Like Cobalt Sulfide Hierarchitectures by Microwave Assisted Heating Method for High-Performance Supercapacitors, Electrochim. Acta 123 (2014) 183.

[46] R. Lin, T. Lin, J. Huang, X. Huang, Y. Liu, Hierarchical Cobalt sulfide with Vertical in-Plane Edge Structure for Enhanced Electrolytic Oxygen Evolution Reaction, Electrochim. Acta 281 (2018) 348.

[47] M. Jin, S.Y. Lu, L. Ma, M.Y. Gan, Y. Lei, X.L. Zhang, G. Fu, P.S. Yang, M.F. Yan, Different Distribution of In-Situ Thin Carbon Layer in Hollow Cobalt Sulfide

Nanocages and Their Application for Supercapacitors, J. Power Sources 341 (2017) 294.
[48] I.M. Babu, J.J. William, G. Muralidharan, Ordered Mesoporous Co_3O_4/CMC Nanoflakes for Superior Cyclic Life and Ultra High Energy Density Supercapacitor, Appl. Surf. Sci. 480 (2019) 371.
[49] C. Yuan, L. Shen, F. Zhang, X. Lu, D. Li, X. Zhang, Interface-Hydrothermal Synthesis and Electrochemical Properties of CoS_x Nanodots/Poly(sodium-4-styrene sulfonate) Functionalized Multi-Walled Carbon Nanotubes Nanocomposite, J. Colloid Interface Sci. 349 (2010) 181.
[50] B. Wang, J. Park, D. Su, C. Wang, H. Ahn, G. Wang, Solvothermal Synthesis of CoS_2-Graphene Nanocomposite Material for High-Performance Supercapacitors, J. Mater. Chem. 22 (2012) 15750.
[51] H. Heydari, M.B. Gholivand, Polyaniline/Reduced Graphene Oxide–Cobalt Sulfide Ternary Composite for High-Performance Supercapacitors, J. Mater. Sci.: Mater. Electron. 28 (2017) 3607.
[52] L. Li, Y. Ding, H. Huang, D. Yu, S. Zhang, H.Y. Cheng, S. Ramakrishna, A. Peng, Controlled Synthesis of Unique Co_9S_8 Nanostructures with Carbon Coating as Advanced Electrode for Solid-State Asymmetric Supercapacitors, J. Colloid Interface Sci. 540 (2019) 389.
[53] Q. Chen, D. Cai, H. Zhan, Construction of Reduced Graphene Oxide Nanofibers and Cobalt Sulfide Nanocomposite for Pseudocapacitors with Enhanced Performance, J. Alloys Compds. 706 (2017) 126.
[54] K. Dai, J. Lv, L. Lu, C. Liang, L. Geng, G. Zhu, Large-Scale Synthesis of Cobalt Sulfide/Carbon Nanotube Hybrid and its Excellent Electrochemical Capacitance Performance, Mat. Lett. 176 (2016) 42.
[55] D. Liu, A. Hu, Y. Zhu, S. Zhou, S. Duan, Q. Tang, Hierarchical Microstructure of CNTs Interwoven Ultrathin Co_3S_4 Nanosheets as High Performance Anode for Sodium-Ion Battery, Ceram. Int. 45 (2019) 3591.
[56] A.G. Tabrizi, N. Arsalani, Z. Naghshbandi, L.S. Ghadimi, A. Mohammadi, Growth of Polyaniline on rGO-Co_3S_4 Nanocomposite for High-Performance Supercapacitor Energy Storage, Int. J. Hydrogen Energy. 43 (2018) 12200.
[57] J.J. William, I.M. Babu, G. Muralidharan, Microwave Assisted Fabrication of L-Arginine Capped α-$Ni(OH)_2$ Microstructures as an Electrode material for High Performance Hybrid Supercapacitors, Mater. Chem. Phys. 224 (2019) 357–368.
[58] I. Rathinamala, I.M. Babu, J.J. William, G. Muralidharan, N. Prithivikumaran, CdS Microspheres as Promising Electrode Materials for High Performance Supercapacitors, Mat. Sci. Semi. Process 105 (2020), 104677.
[59] D.P. Dubal, G.S. Gund, C.D. Lokhande, R. Holze, Controlled Growth of CoS_x Nanostrip Arrays (CoS_x-NSA) on Nickel Foam for Asymmetric Supercapacitors, Energy Technol 2 (2014) 401.
[60] S.J. Patil, J.H. Kim, D.W. Lee, Graphene-Nanosheet Wrapped Cobalt Sulphide as a Binder Free Electrode for Asymmetric Solid-State Supercapacitor, J. Power Sources 342 (2017) 652–666.
[61] J. Shi, X. Li, G. He, L. Zhang, M. Li, Electrodeposition of High-Capacitance 3D CoS/Graphene Nanosheet on Nickel Foam for High Performance Aqueous Asymmetric Supercapacitor, J. Mater. Chem. A 3 (2015) 20619–20626.
[62] R.B. Rakhi, N.A. Alhebshi, D.H. Anum, H.N. Alshareef, Nanostructured Cobalt-Sulfide-on-Fiber with Tunable Morphology as Electrodes for Asymmetric Hybrid Supercapacitors, J. Mater. Chem. A 2 (2014) 16190.